Automated Detection of Primary Liver Cancer using Different Deep Learning Approaches

Kamel H.Rahoma[1], Hoda Anwar A.Ibrahim[2*], Mohamed A. Massoud[2]

[1]Department of Electrical Engineering, Minia University, Minia 61111, Egypt.

[2]Department of Biomedical Engineering, Minia University, Minia, 61519, Egypt.

*Corresponding author(s). E-mail(s): h.anwar@mu.edu.eg.

Abstract

Hepatocellular carcinoma (HCC) is the world's sixth-most common malignancy and the fourth-leading cause of cancer death. This paper introduces an early diagnose to HCC using fully autonomous system by artificial intelligence (AI) techniques. This system consists of three stages; preprocessing, liver segmentation, and classifier stage.Preprocessing improves the quality of the abdominal Computed Tomography(CT) scan to be better analyzed. The liver is extracted and segmented from improving CT image using various deep learning techniques, and semantic segmentation is used to separate lesions from a tumor-filled liver in cases of HCC by classifier. U-Net and Resnet50 deep learning algorithms are used to segment the liver and tumour automatically, but the Resnet50 achived the better results with a DICE score of 0.926, and loss of 0.0028. The classifier's robustness is justified using 5-fold cross-validation (CV). The Resnet 50 classifier, which is a classification approach based on transfer learning (TL), achieved 96% accuracy for the binary classifier. In comparison with the linked methods, the proposed system confirms that it is the promised fully autonomous system for liver segmentation and tumour segmentation in cases diagnosed with HCC.

1. Introduction

According to World Health Organization data liver cancer is the second most common cause of mortality in males and the sixth most common cause of death in women [1]. Egypt is the world's third and fifteenth most populous country, respectively. [2]. In order to increase opportunities, Non-invasive diagnosis of liver lesions could be assessed by using CT. Abdominal CT scans are considered one of the most widely used medical imaging modalities featured in their fast-scanning speed and high spatial resolution for detecting and diagnosing liver abnormalities. For the mortality rate to be reduced, early detection is necessary. Images are acquired both before and after intravenous injection of contrast material, and lesions are best seen in portal phase images (60-80 seconds after injection). However, the liver is only visually inspected during modern radiation therapy. It takes a long time and is tedious to visually inspect a large number of tumors and liver organs from a CT scan [3]. To accomplish the segmentation task, a clinician's or doctor's experience is crucial. The liver organ varies significantly in size and shape from human to patient. The task of early segmentation and detection of liver lesions is

quite demanding and takes many steps to find an answer. Some challenges can be highlighted as follows:

1. The difference in contrast between healthy tissue and existing tumor tissue is very small. Furthermore, the difference in contrast differs from situation to situation.

2. The form and location of the liver vary greatly between individuals.

3. Organs other than the liver are found in the CT scan of the abdomen and must be removed [1].

Traditionally, radiologists have to look at CT scans of the liver one by one to find liver tumors, which not only takes a lot of time and effort, but also makes it easy to make mistakes due to fatigue or subjective judgment. Hence, there is an urgent need for automated liver tumor detection and segmentation algorithms to assist clinicians[2].

The purpose of this paper is to carry out the segmentation and early diagnosis of hepatic cancer. This will be done by applying DICOM data segmentation on the liver CT or MRI images. This will be based on U-Net artificial intelligence technique after preprocessing of the obtained liver CT and MRI images. The

paper has been divided into five sections. Section (1) provides an introduction, while Section (2) is a survey of the literature review. Section (3) describes the techniques used in this study, and Section (4) depicts the experiment and results. It also explores these findings and compares them to other research findings. Section (5) summarizes some conclusions and proposes some areas for future research. A list of the references used is provided at the end of the study.

2. Related Work

This section introduces a review of a wide range of current articles on biomedical image analysis for liver cancer preprocessing, segmentation, and diagnosis. After extracting the CT liver border using first order statistical characteristics of the liver image, the authors employed a k-Mean classifier based on distance and color to categorize lesions in [6]. The tumors were segmented and categorized as benign or malignant in [7] using a binary logistic regression analysis based on the extraction of texture, shape, and kinetic curve data (a region-expanding technique). Traditional approaches have a disadvantage in that the retrieved features may not be sufficient to detect the complexity of the tumor segmentation challenge. As a result, more complex traits must be studied. In the past few years, a lot of research has focused on liver or tumor segmentation and classification using supervised learning techniques. These learning methodologies are topped by deep learning techniques [8],[9]. The Stacked Autoencoder (SAE), Deep Belief Net (DBN), Convolutional Neural Network (CNN), and Deep Boltzmann Machine (DBM) are a few further deep learning models [10],[11]. The work described in [12] demonstrated a greater than 94% percent accuracy rate for categorizing the images as normal or abnormal when the image showed a liver with tumor areas. The two-dimensional (2D) U-Net, which is primarily employed in medical picture segmentation, was utilized in other investigations [13], [14]. Authors, in [15], used a segmentation framework that included a preprocessing step, pixel-wise classification using a pre-trained CNN (Alexnet), and smoothing and thresholding as a post-processing step to get binary segmented images. Utilizing the VGG Segnet model, [16] attempted to segment the liver and lesion in more than one stage using cascaded deep learning algorithms. Two cascaded VGG16 models were used in the research in [17], the first of which produced segmentations of the liver and served as input for the second VGG16 model, which produced segmentations of the lesions. The authors of [18] used a two cascaded fully convolutional networks (Unet-like) model for combined segmentation of the liver and lesions from CT images. The model [19] was built using end-to-end training to segment the liver and lesions. The authors of [20] used a deep residual network (Resnet) [21],[22] used a CNN model to autonomously separate the liver lesions.

To overcome a lack of image data, TL, a practical deep learning technique, is applied. TL has proven to be a very successful strategy, particularly when working with constrained medical pictures [23]. The models were used to differentiate the components of medical images much more quickly and with a lot less training data [24]. Utilizing pre-trained CNNs, TL has an advantage over traditional deep learning algorithms that use untrained CNNs in that it can achieve better classification accuracy with a small dataset [25]. Several studies [26],[27] have established the utility of TL with pre-trained CNNs for liver cancer. Furthermore, authors in [28] used CT scans converted to Jpeg format to classify liver masses (cell masses). In image classification and detection challenges, deep residual networks (ResNet) of 50, 100, 150, or 1000 layers have obtained state-of-the-art results. ResNet architectures are made up of a number of residual blocks that bypasses(skips or shortcuts) a few convolution layers at a time[29]. The outputs of the shortcut connections are combined with the outputs of the convolution layers, overcoming the limitation of adding more layers by lowering the training degradation seen in deep networks [20].

By discussing recent advances in the early detection, management, and prevention of HCC. The use of newer imaging techniques, such as Magnetic resonance imaging (MRI) and contrast-enhanced ultrasound, along with image segmentation technology and deep learning models, have greatly enhanced the accuracy of HCC detection and diagnosis[30]. A new computer-aided design (CAD) system that utilizes CNN and TL, specifically pre-trained VGG-16 and MobileNet-V1 models presented in [31] . In [32] showed machine learning algorithms for diagnosis of HCC and mentioned many tested lab for HCC.

However, better approaches to improve accuracy and dice coefficient are needed to be investigated. The suggested framework here accomplishes this goal by establishing a

comparison between deep learning algorithms, such as Unet and Modified ResNet models, that have proven success for liver cross-sectional CT scans segmentation and find the best one based on model efficiency in rapidly and accurately segment abdominal CT. Also, TL technique is used for better classification.

3. Materials and Method

This paper aims to early diagnose HCC using artificial intelligence techniques Fig. 1. Illustrates the block diagram of the proposed method for
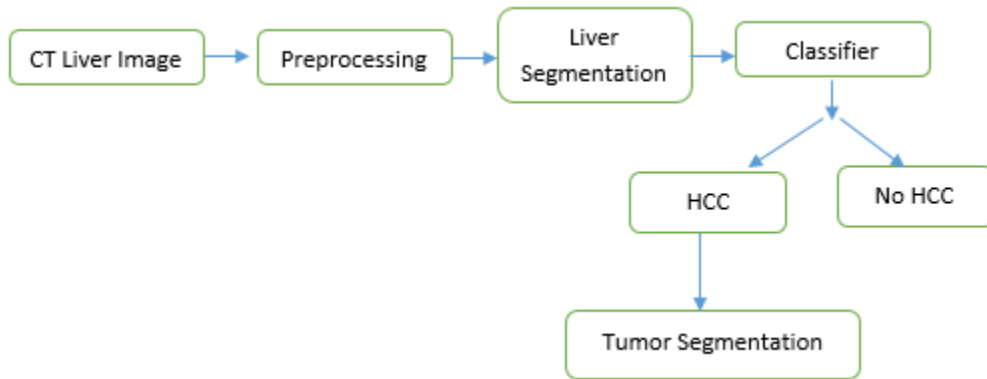
Figure 1. Block diagram of the proposed method for classifying hepatocellular carcinoma.

3.1. CT liver image:

The 3D-IRCADb-01 DICOM format database in [33] is used in the input stage. It consists of three-dimensional (3D) CT scans of 20 different patients (10 women and 10 men), 15 of them have liver tumors with 512×512 image resolution, and the slices for each patient ranges from 74 to 260.

Python language and Keras with the TensorFlow backend are used in the proposed network. The Nvidia Quadro K2200 as the GPU and Intel Xenon® processor with 3.2 GHz clock speed as the CPU are used in our hardware.

3.2. Preprocessing and settings:

Preprocessing stage is a very important stage. In this stage the DICOM CT scans will pass

through four substages namely: Hounsfield Windowing, Reducing Noise, Contrast Enhancement, and Resize Images.

3.2.1 Hounsfield Windowing (HU):

When segmenting the liver, Hounsfield Unit Range is utilized [34]. Utilizing Hounsfield Windowing, the liver's intensity range is highlighted while non-relevant organs are excluded. The HU windowing employed in this study is [100,400] and is applied to datasets used in the FCN training phase for both liver segmentation methods.

3.2.2 Reducing Noise:

After applying HU windowing DICOM images are converted to jpg or png images and they

can be handled as a gray scale image. To eliminate noise, a gaussian smoothing filter is used. The continuous Gaussian function (centered at x = µ) is continuous in one dimension.

$$g(x) = \frac{1}{\sigma\sqrt{2\pi}}\, e^{-0.5(\frac{xi-\mu}{\sigma})^2} \qquad (1)$$

Where x is the filtered point's location, (µ) is the mean, and (σ) is the standard deviation. The continuous Gaussian function (centered at (µ)) in two dimensions is

$$F(x,y) = \frac{1}{2\pi\sigma^2}\, e^{-((x-\mu x)^2 + \frac{(y-\mu y)^2}{(2\sigma^2)})} \qquad (2)$$

Where (x,y) represent the filtered point's 2D position. Because the filtering is done with a mask, the weights are calculated in Equation 1-2 using row and column coordinates (with respect to the pixel locations) as the x and y inputs [35].

3.2.3 Contrast Enhancement:

Adaptive histogram equalization is a contrast enhancement approach. It creates numerous histograms for different image portions and then uses these image sections to redistribute the image's brightness value. It is useful for improving visual perception in low-contrast images [36].

3.2.4 Resize Images:

Preprocessed images are resized according to the required shape of the training model. Testing datasets are passed to the same preprocessing sequence.

3.3. Liver Segmentation:

Liver Segmentation phase is the second stage after preprocessing. In this stage the deep learning techniques are used. Liver Segmentation accomplished by two methods: U-Net and ResNet models.

ResNet and U-Net differ in structure only, but their hyper parameters are the same. Both networks are trained from scratch with 15 epochs (batch size = 4). Adam Optimizer is used to update network parameters with 0.0001 learning rate. Also, callback and early stopping methods are used.

After preprocessing step, all training slices are resized to have a common size, so the inputs to each of the Fully connected network (FCNs) are 256×256 (2D) grayscale slices, and their outputs are 256×256 binary mask images.

The first network is trained to separate the liver envelope from the background using abdominal slices, and the abdominal slices are then resampled to the input size (256 x 256). Given the liver envelope image, train the second network to segment the tumor. The liver Region of interest (ROI) helps to reduce the percentage of non-tumor pixels that are misclassified. The second ResNet focuses on learning the features that distinguish the tumor from the liver background segmentation.

3.3.1 The U-Net model

The network architecture is formed like a U. There are three components to the U-Net architecture. The first part of the down sampling path consists of two convolutional layers, followed by a max-pooling layer with a window size of (2*2) and a stride value of 2. The input liver image is convolved twice with a filter of size (3*3) before applying a ReLU activation function. Because the output image will have the same dimensions as the original image, the padding value is kept constant.

The first group's convolution layer's filter number is set to eight, and it doubles for each subsequent layer group until it reaches the fifth. Following that, an up-sampling path is taken in which the feature maps of each group are half.

In order to do this, the U-Net architecture employs a concatenation layer, which has the same number of filters as the current layer group, to combine the features from the down-sampling layer and the layer before it.

A ReLU activation function comes after a convolutional filter of size (3*3) in two layers. This layer group is repeated from group six to group nine. The output layer is the eleventh layer, a convolutional one with a (1*1) filter and eight feature channels. This architecture has 27 layers in total (18 convolutional + ReLU, 4 pooling, 4 up convolutional, and 1 SoftMax). The U-Net design is depicted in Fig. 2 [4].
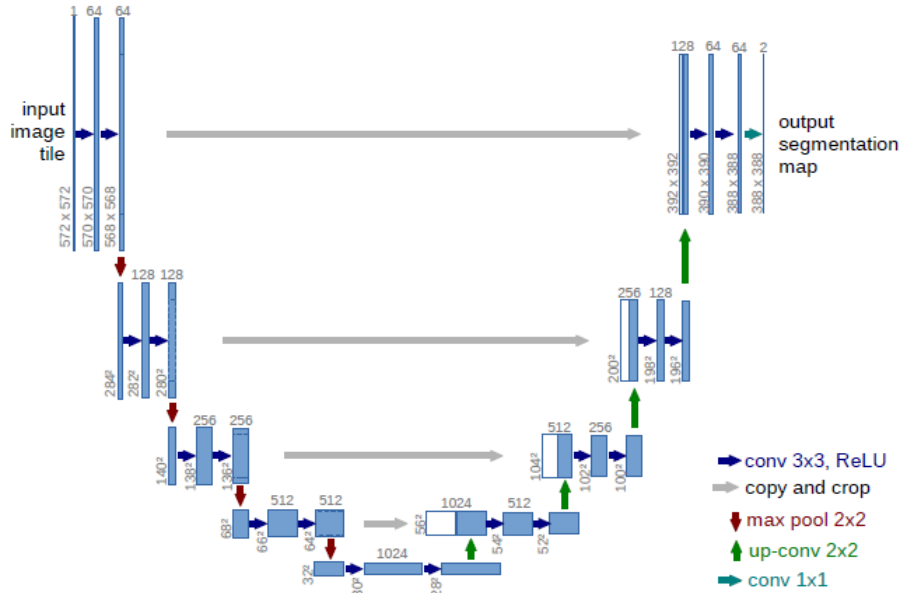
Figure 2. The Unet configuration

3.3.2 The ResNet Model

The second model is ResNet where it replaces convolution blocks of the U-Net with residual blocks giving us the advantages of both models.

The depth of the network is quite important. A extremely deep neural network, however, frequently undergoes gradient vanishing during back propagation, which has a negative impact on training outcomes. To solve this issue, [29] suggested using a deep residual learning framework to learn the identity map's residual.

The stacked residual blocks at the structural level of the neural network solve the gradient vanishing problem by employing identity mappings as the skip connections.

Three sets of combinations of a batch normalization (BN) layer, an activation (ReLU) layer, and a convolutional layer make up the residual block.

As the network becomes "deeper," a convolutional identity mapping connection is utilized to guarantee accuracy. Fig. 3 [37] provides a comprehensive illustration of the residual unit.
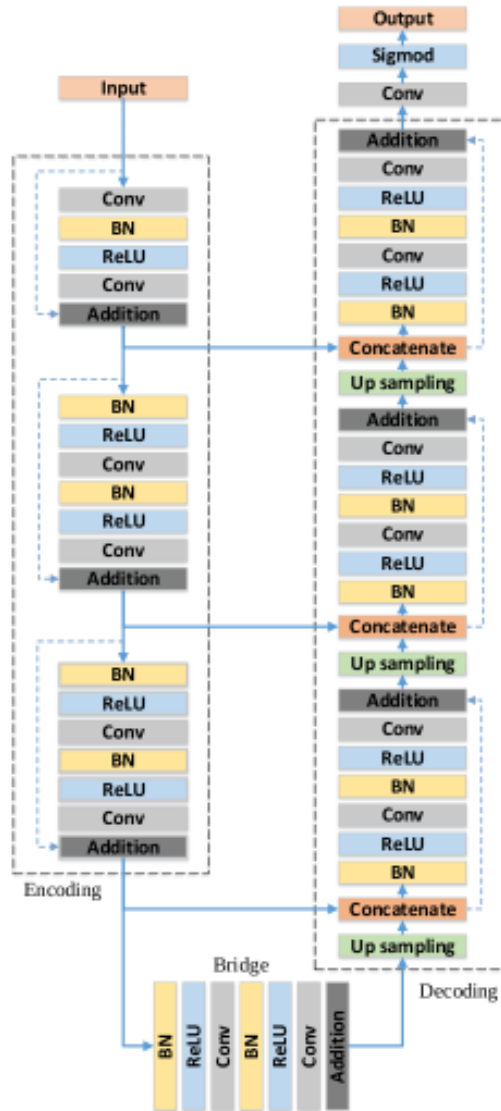
Figure 3. The ResNet configuration

3.4 Classifier

In this stage transfer learning models are used for classification.

Pretrained Models:

To categorize CT scans the Residual50 is used to speed up the training and testing procedures and improve overall accuracy and reduce error rate. Fig. 4 illustrates transfer learning block diagram. Fig. 5 depicts the proposed deep neural network (DNN) model, It includes the following four fundamental procedures: (i) Preparing data (DP), (ii) pre-trained model (PT), (iii) extraction of the features (FS), and (iv) classifier and loss function (CL).
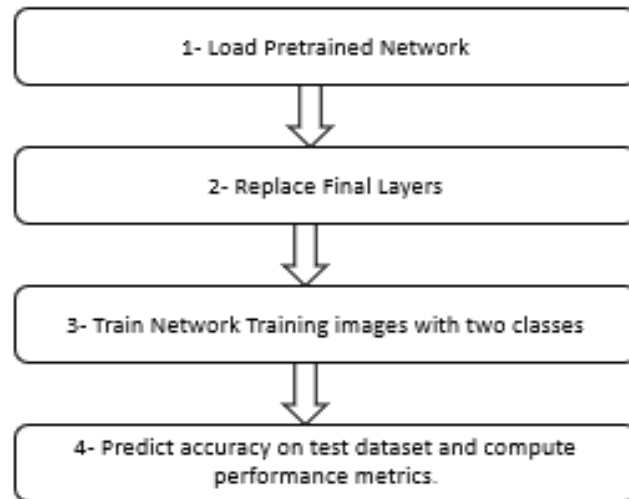
Figure 4. Transfer Learning Mechanism.
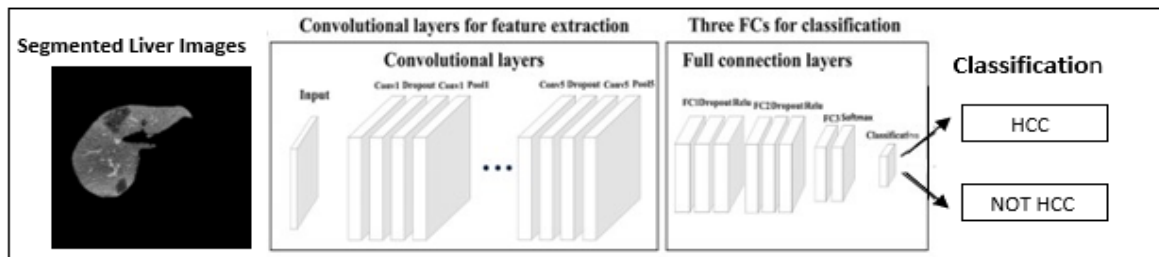
Figure 5.   The proposed DNN model for classifying hepatocellular carcinoma.

3.4.1. Data Preparation:

Data preparation includes three rounds: resize images, Data augmentation and validation.

(i) Images resize:

Segmented liver images from CT scans are resized to match ResNet50 Pretrained Model as desired input size.

(ii) Data augmentation:

Data augmentation is a technique for artificially expanding the dataset and avoiding model overfitting. It is introduced before the training procedure. In our study data augmentation includes rotation, reflection, and shearing.

(iii) Validation:

Data partitioning into training and testing sets using k-fold cross validation method with k=5. Validation and testing data are resized by 224*224*3. The validation accuracy provides an estimate of how well the model is likely to perform on unseen data.

3.4.2 Residual neural network transfer

learning:

A deep convolutional neural network with representative image auto-encoding and classification is called ResNet50. The classifier stage network is built from a 50-layer residual network architecture, has 177 layers overall, 5-fold cross-validation on two classification groups, 10 iterations, 8 mini batches, and a stochastic gradient descent optimizer with a learning rate of 0.0001.

Figure 6 illustrates the ResNet50 architecture and a deep learning flowchart for CT images. In the pretrained network, the weights of earlier layers (1-174) were frozen. The parameters of the frozen layer are not adjusted by the training network. It is feasible to freeze the weights of numerous initial layers to expedite network training and prevent over-fitting to a new batch of medical data.

The last three convolutional layers are replaced by new layers in a sequence of blocks in order to extract deep residual features and transfer features from the front layer to the later one. At the network's end, classification is carried out via a full connection layer. During training, weights were adjusted using the stochastic gradient descent (SGD) optimization algorithm with a 64-piece mini-batch size [29]. The maximum epochs and learning rate are adjusted to 10 and 0.0001 respectively, after fine-tuning deep learning parameters to guarantee that the whole data is covered for efficient training. Binary cross-entropy is discovered as the loss function. Before the output layer, we utilize the sigmoid function to compute the probability. AUC and accuracy are used to assess the deep learning model's performance[38].
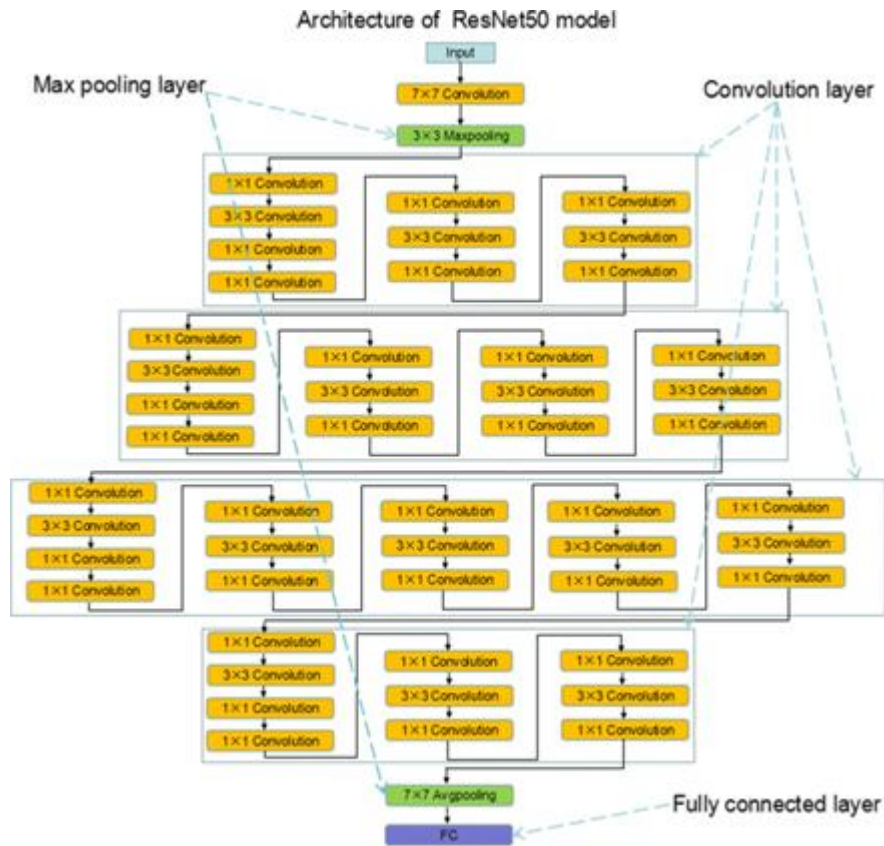
Figure 6. ResNet50 Architecture

3.5. Performance measure (Quantitative

Evaluation Metrics):

The adequacy of the proposed approach is measured by; true positive rate, intersection over union, precision, and F1 score.

1) Recall (Re) or true positive rate (TPR): As expressed in Equation (4) , these terms refer to the system's ability to recognize tumor pixels properly in relation to the total number of true tumor pixels.

$$\text{Re} = \frac{TP}{TP+FN} \qquad (4)$$

2) Intersection over union (IoU): this is the proportion of pixels that have been correctly classified to the sum of the anticipated and actual pixels for a given class. Equation (5) shows the formulation of

$$\text{IoU} = \frac{TP}{TP+FP+FN} \qquad (5)$$

3) Precision (Pr): represents the level of confidence in the tumor prediction made for the predicted positive class. It is expressed as follows in Equation (6):

$$\text{Pr} = \frac{TP}{TP+FP} \qquad (6)$$ **4) F1 score (F1):** According to Equation (7) , The arithmetic

mean of recall (true positive rate) and precision is the F1 score (F1). It checks whether a position on the expected boundary corresponds to a point on the actual border:

$$\text{F1} = \frac{2(Pr*Re)}{Pr+Re} \qquad (7)$$

5) Overall Accuracy: Overall Accuracy: This measures the proportion of accurately categorized pixels to all pixels. This could take the form of Equation (8):

$$\text{Accuracy} = \frac{TP+TN}{TP+FP+TN+FN} \quad (8)$$

3. Results

A new autonomous system to extract the liver and tumor from a CT scan of the abdomen is introduced. This system is designed for liver, tumor segmentation and diagnosed livers with Hepatocellular Carcinoma. The main stages in this system are preprocessing, liver Segmentation and classification stage.

.
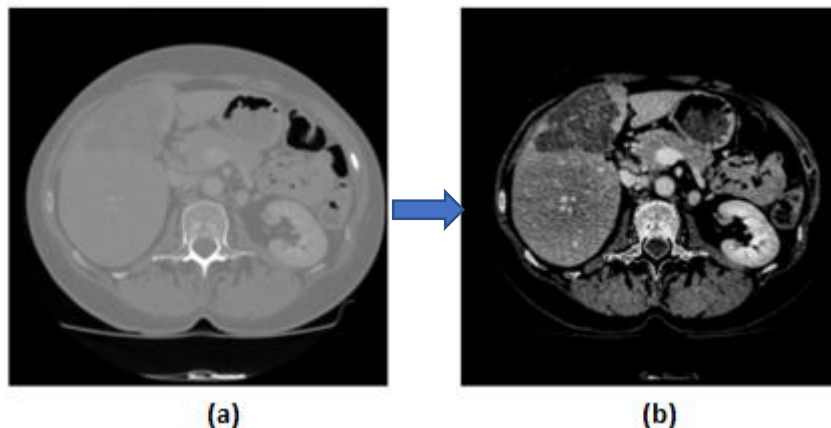
Figure 7. a) Abdominal CT scan, b) Preprocessed Image.

Fig. 7 shows the huge effect of preprocessing stage. The fuzzy and hazy boundaries are improved and enhanced in the preprocessing stage.
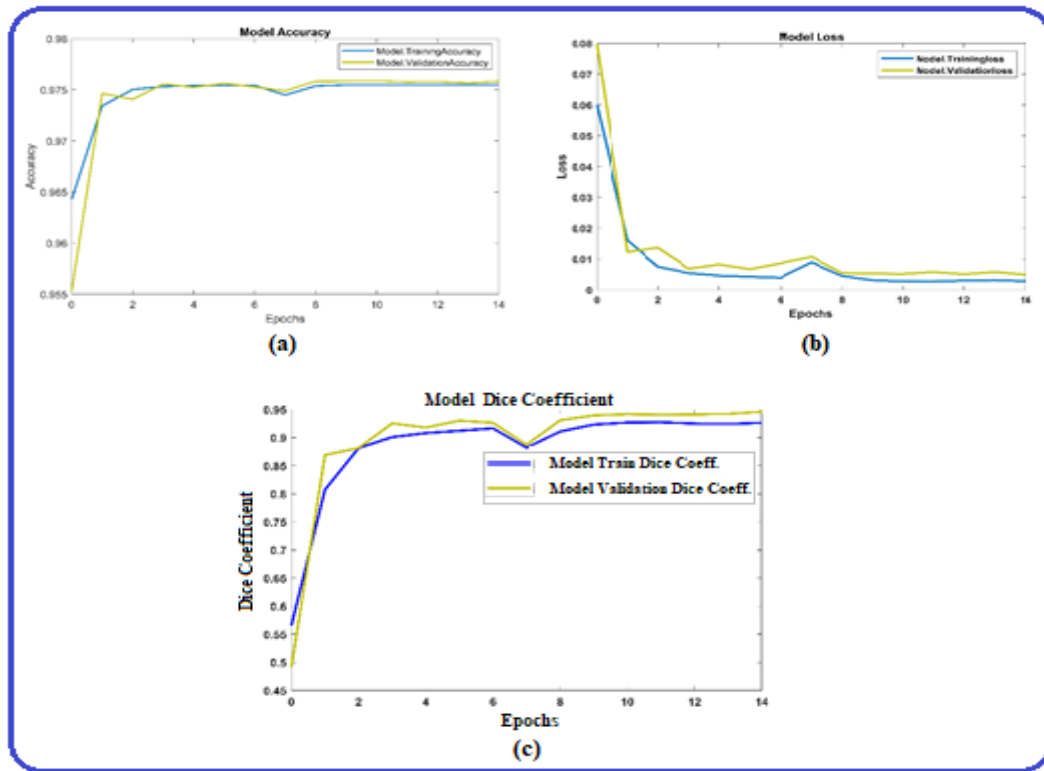
Figure 8. (a); The model accuracy, (b); Loss for training and validation, and (c); The model DSC for training and validation data.
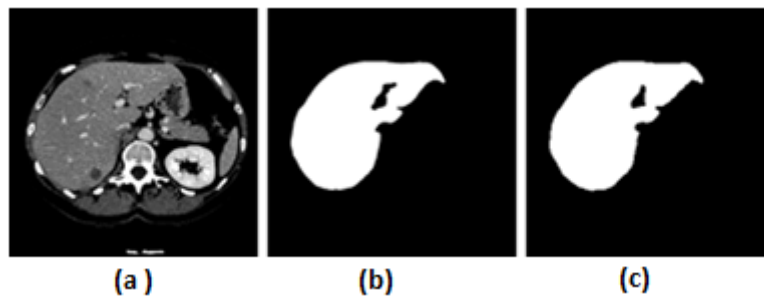
Figure 9. a) Abdominal CT b) Liver segmentation ground truth and c) Liver Segmentation results using Resnet
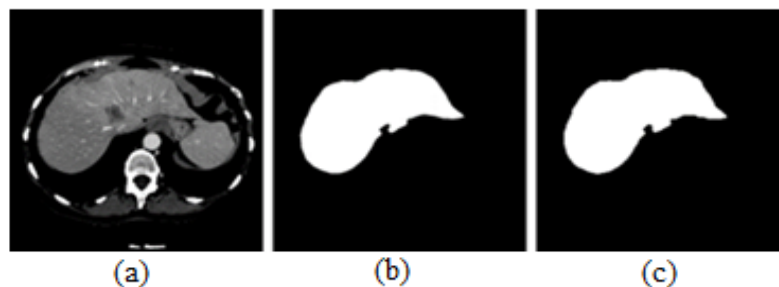
Figure 10. a) Abdominal CT, b) Liver segmentation ground truth, and c) Liver Segmentation results using Unet
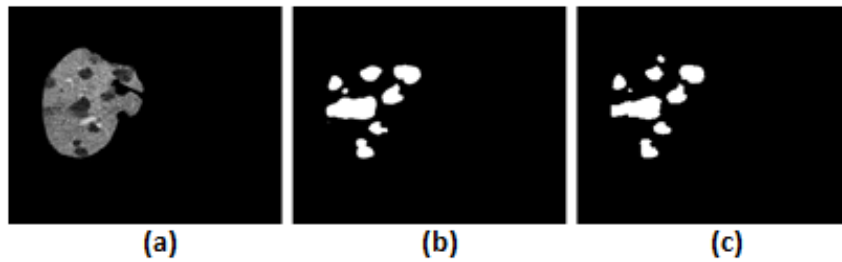
Figure 11. a) Segmented Liver, b) Tumor segmentation ground truth, and c) Tumor Segmentation results using Resnet.

Fig. 8 illustrates the model accuracy, loses and DSC of training and validation. The results of the segmentation algorithms along with input images and ground truths are included in Fig. 9 and Fig 10 using Resnet and Unet respectively. Fig.11 shows the segmented liver as well as the tumor segmentation ground truth and the tumor segmentation resulted from the ResNet. Fig. 11 shows that the fine and tiny tumors are segmented carefully. Fig. 12 compares the Dice coefficients and losses of the two models.
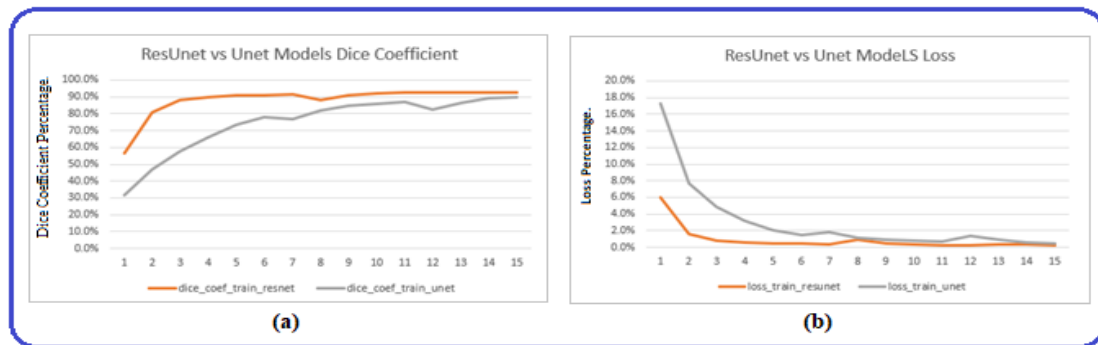
Figure 12: Resnet vs Unet Dice Coefficient and Loss Comparison.

Comparison between ResNet and U-Net results

The paper's main contribution is that ResNet surpasses U-Net in terms of liver extraction, with a DICE score of 0.926 versus 0.897, and with loss of 0.0028 versus 0.0049. Also, ResNet surpasses U-Net in terms of tumor segmentation with a DICE score of 0.66 versus 0.367. and with loss of 0.001 versus 0.01. From the previous results and graphs of Fig.12 it can be concluded that the ResNet model is better and more accurate than U-Net model for both liver and tumor segmentation. So that the ResNet model is recommended to be used.

Classification Results:

After passing the segmented liver image to the ResNet 50 classifier, the model achieved an accuracy of 96%. Table I gives a summary of classifier performance evaluation results. Fig. 13 shows Resnet result: (a) Accuracy (b) Loss (c) Confusion Matrix and (d) AUC. The training and validation accuracy are represented, respectively, by the blue and light blue lines. Additionally, the orange and light orange lines show the corresponding losses from training and validation.
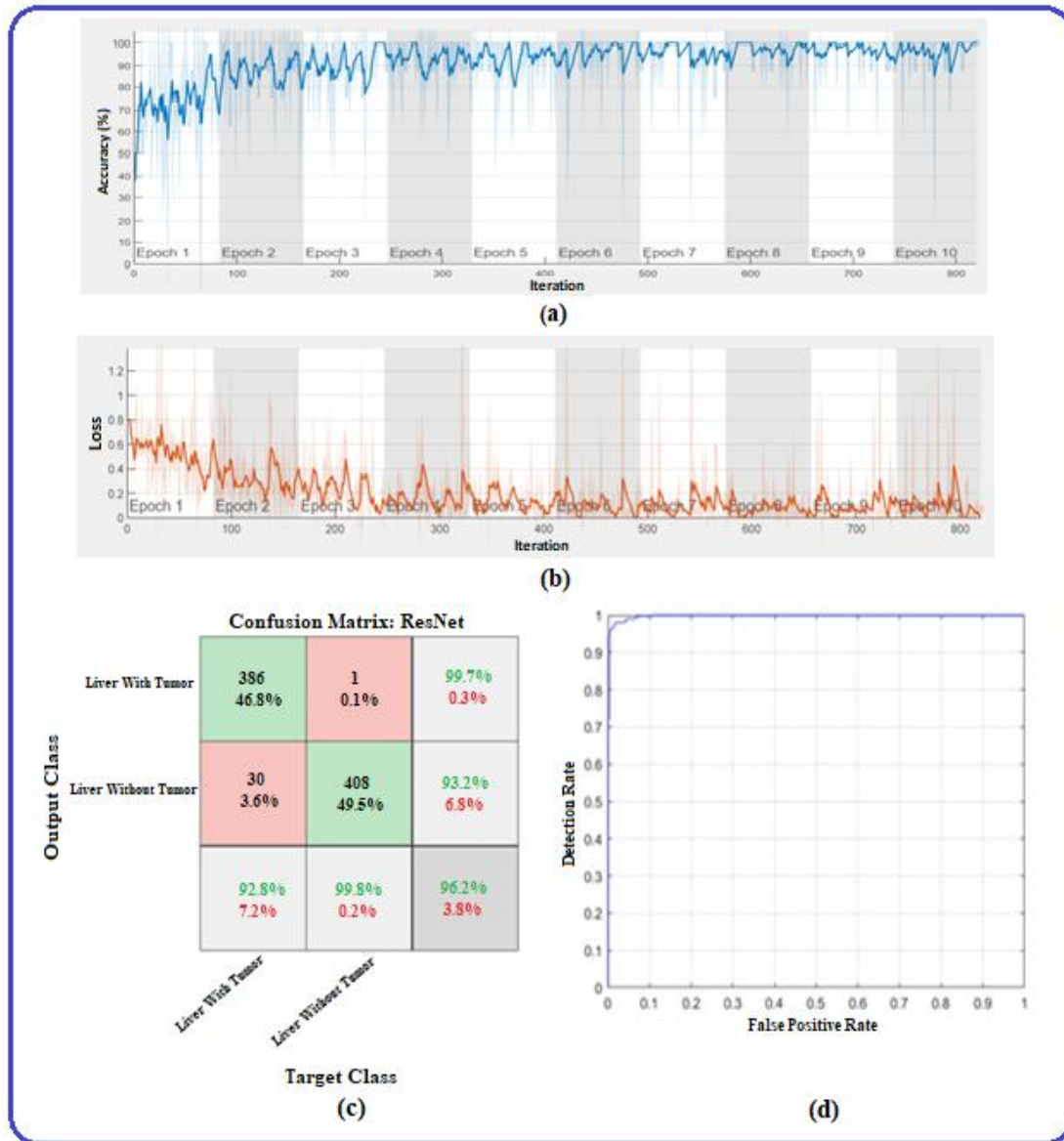
Figure 13: The Resnet results: (a) Accuracy (b) Loss (c) Confusion Matrix and (d) AUC.

TABLE I

SUMMARY OF CLASSIFICATION RESULTS OBTAINED BY 5-FOLD CROSS-VALIDATION ON TWO CLASSIFICATION GROUPS.

ACCURACY	SENSITIVITY	SPECIFICITY	PRECISION	RECALL	F-MEASURE	AUC
0.962424	0.927885	0.997555	0.997416	0.927885	0.961395	0.997931

Liver and lesion segmentation dice scores and accuracy are studied with other works. Tables II and III show the dice coefficient scores for the segmentation of the liver and tumor, respectively. Table IV shows accuracy comparison for cascaded liver and tumor segmentation.

TABLE II

Comparison of dice coefficient among three algorithms for liver segmentation.

AUTHORS (S)	DATASET USED	DICE SCORE
KALUVA[39]	LITS	91.2%
AHMAD[40]	3DIRCADB	91.8%
PROPOSED METHOD	3DIRCADB	92.6%

TABLE III

COMPARISON OF DICE COEFFICIENT AMONG THE PROPOSED ALGORITHM AND OTHER ALGORITHMS FOR LESION SEGMENTATION.

AUTHORS (S)	DATASET USED	DICE SCORE
BI[20]	LITS	64.5%
YUAN[41]	LITS	65.7%
KALUVA[39]	LITS	49%
CHRIST[12]	3DIRCADB	56%
PROPOSED METHOD	3DIRCADB	66%

TABLE V I

COMPARISON ON THE OVERALL ACCURACY FOR THE PROPOSED ALGORITHM AGAINST OTHER WORK.

AUTHOR (S)	METHOD	ACCURACY
CHEBUS[42]	RANDOM FOREST	90%
CHRIST[12]	CASCADED FULLY CONVOLUTIONAL NEURAL NETWORKS (CFCNS) WITH DENSE 3D CONDITIONAL RANDOM FIELDS (CRFS)	94%
YANG[43]	A DEEP IMAGE-TO-IMAGE NETWORK (DI2IN)	95%
BI[20]	DEEP RESIDUAL NETWORK (CASCADED RESNET)	95.9%
LI[44]	H-DENSEUNET	96.5%
YUAN[41]	HIERARCHICAL CONVOLUTIONAL— DECONVOLUTIONAL NEURAL NETWORKS	96.7%
WEN LI ET AL[10]	CONVENTIONAL CONVOLUTIONAL NEURAL NETWORK (CNN)	80.6%
OUR METHOD	**CASCADED RESNET**	**97.54%**

From dice scores shown in Table III, Tumor segmentation dice score for our proposed model

around 66%, which is considered a better dice value compared with other models.

Figure 14. Comparison results for : (a) Liver segmentation (b) Lesion segmentation (c) Overall accuray.

Where LiTS dataset is converted from NIFTI (Neuroimaging Informatics Technology Initiative) to DICOM format to be used in our system. Fig. 12 shows bar chart for each table illustrated above.

5. Conclusion

• This paper introduces a fully automated system that diagnoses primary malignant hepatic tumors after segmenting liver envelopes from abdominal CT scans. The fully automated system is the main advantage of this study compared with all studies before, which were limited to either segmentation or classification stages only.

• ResNet surpasses U-Net in terms of liver feature extraction, with a DICE score of 0.926 versus

0.897 and a loss of 0.0028 versus 0.0049. Also, ResNet surpasses U-Net in terms of tumor segmentation, with a DICE score of 0.66 versus 0.367 and a loss of 0.001 versus 0.01.

• This system has also good results in classification in accuracy, sensitivity, and precision (0.962424, 0.927885, and 0.997416) respectively.

• By comparing this system with other works illustrated in this paper, it achieves liver and lesion segmentation with 92.6% and 66% of DICE scores. Besides, it scores 97.54% in classification accuracy. Moreover, the promising system can segment the fine and tiny tumors carefully with good accuracy.

References

[1] H. Sung et al. :Global Cancer Statistics 2020: GLOBOCAN Estimates of Incidence and Mortality Worldwide for 36 Cancers in 185 Countries. CA. Cancer J. Clin. vol. 71, no. 3, pp. 209–249. 2021. doi: 10.3322/caac.21660.

[2] W. M. Rashed, M. A. M. Kandeil, M. O. Mahmoud, and S. Ezzat. :Hepatocellular Carcinoma (HCC) in Egypt: A comprehensive overview. J. Egypt. Natl. Canc. Inst. vol. 32, no. 1. 2020.doi: 10.1186/s43046-020-0016-x.

[3] R. M. Ghoniem.:A Novel Bio-Inspired Deep Learning Approach for Liver Cancer Diagnosis. Inf., vol. 11, no. 2. 2020. doi: 10.3390/info11020080.

[4] N. Nanda, P. Kakkar, and S. Nagpal.:Computer-Aided Segmentation of Liver Lesions in CT Scans Using Cascaded Convolutional Neural Networks and Genetically Optimised Classifier. Arab. J. Sci. Eng. vol. 44, no. 4, pp. 4049–4062. 2019. doi: 10.1007/s13369-019-03735-8.

[5] L. Meng, Q. Zhang, and S. Bu.:Two-stage liver and tumor segmentation algorithm based on convolutional neural network. Diagnostics. vol. 11, no. 10. 2021. doi: 10.3390/diagnostics11101806.

[6] A. H. Ali, E. M. Hadi, and S. N. Mazhir.:Diagnosis of Liver Tumor from CT Images using Unsupervised Classification with geometrical and Statistical features. Int. J. Adv. Res. Comput. Sci. Softw. Eng., vol. 5, no. 3, pp. 28–35, 2015.

[7] C. C. Chang et al. :Computer-aided diagnosis of liver tumors on computed tomography images. Comput. Methods Programs Biomed., vol. 145, pp. 45–51, 2017, doi: 10.1016/j.cmpb.2017.04.008.

[8] S. Almotairi, G. Kareem, M. Aouf, B. Almutairi, and M. A. M. Salem.:Liver tumor segmentation in CT scans using modified segnet. Sensors (Switzerland), vol. 20, no. 5, 2020, doi: 10.3390/s20051516.

[9] Z. C. Horn, L. Auret, J. T. McCoy, C. Aldrich, and B. M. Herbst.:Performance of Convolutional Neural Networks for Feature Extraction in Froth Flotation Sensing. IFAC-PapersOnLine, vol. 50, no. 2, pp. 13–18, 2017, doi: 10.1016/j.ifacol.2017.12.003.

[10] W. Li, F. Jia, and Q. Hu.:Automatic Segmentation of Liver Tumor in CT Images with Deep Convolutional Neural Networks. J. Comput. Commun., vol. 03, no. 11, pp. 146–151, 2015, doi: 10.4236/jcc.2015.311023.

[11] M. Rajeshwaran and A. Ahila.: Segmentation of Liver Cancer using SVM. Original images Image Pre-processing Using Gabor filter Segmentation. Int. J.Comput. Commun. Inf. Syst.(IJCCIS), vol. 6, no. 2, pp. 78–80, 2014.

[12] P. F. Christ et al.:Automatic liver and lesion segmentation in CT using cascaded fully convolutional neural networks and 3D conditional random fields. Lect. Notes Comput. Sci. (including Subser. Lect. Notes Artif. Intell. Lect. Notes Bioinformatics), vol. 9901 LNCS, pp. 415–423, 2016, doi: 10.1007/978-3-319-46723-8_48.

[13] U. States, G. Carneiro, and A. P. Bradley. for publication in the following source : FULLY AUTOMATED CLASSIFICATION OF MAMMOGRAMS USING DEEP RESIDUA. Australian Centre for Visual Technologies , The University of Adelaide School of ITEE , The University of Queensland," pp. 310–314, 2017.

[14] H. Lin et al.:Automated classification of hepatocellular carcinoma differentiation using multiphoton microscopy and deep learning. J. Biophotonics, vol. 12, no. 7, 2019, doi: 10.1002/jbio.201800435.

[15] A. N. Korabelnikov, A. V. Kolsanov, S. S. Chaplygin, P. M. Zelter, K. V.

Bychenkov, and A. V. Nikonorov.:Liver tumor segmentation ct data based on Alexnet-like convolution neural nets. CEUR Workshop Proc., vol. 1638, no. January 2017, pp. 348–356, 2016, doi: 10.18287/1613-0073-2015-1638-348-356.

[16] V. Badrinarayanan, A. Kendall, and R. Cipolla.:SegNet: A Deep Convolutional Encoder-Decoder Architecture for Image Segmentation. IEEE Trans. Pattern Anal. Mach. Intell., vol. 39, no. 12, pp. 2481–2495, 2017, doi: 10.1109/TPAMI.2016.2644615.

[17] M. Bellver, K.-K. Maninis, J. Pont-Tuset, X. Giro-i-Nieto, J. Torres, and L. Van Gool.:Detection-aided liver lesion segmentation using deep learning. no. Nips, 2017, [Online]. Available: http://arxiv.org/abs/1711.11069.

[18] E. Vorontsov, A. Tang, C. Pal, and S. Kadoury.:Liver lesion segmentation informed by joint liver segmentation. Proc. - Int. Symp. Biomed. Imaging, vol. 2018-April, pp. 1332–1335, 2018, doi: 10.1109/ISBI.2018.8363817.

[19] O. Ronneberger, P. Fischer, and T. Brox.:U-Net: Convolutional Networks for Biomedical Image Segmentation.pp. 1–8.

[20] L. Bi, J. Kim, A. Kumar, and D. Feng.:Automatic Liver Lesion Detection using Cascaded Deep Residual Networks. 2017, [Online]. Available: http://arxiv.org/abs/1704.02703.

[21] M. M. B, A. Sarti, S. Tubaro, D. Elettronica, I. Bioingegneria, and P. Milano.:Computer Vision – ECCV 2016. vol. 9905, pp. 480–494, 2016, doi: 10.1007/978-3-319-46448-0.

[22] G. Litjens et al.:A survey on deep learning in medical image analysis. Med. Image Anal., vol. 42, no. 1995, pp. 60–88, 2017, doi: 10.1016/j.media.2017.07.005.

[23] H. Shin et al.:Deep Convolutional Neural Networks for Computer-Aided Detection : CNN Architectures , Dataset Characteristics and Transfer Learning. pp. 1–14, 2016, doi: 10.1109/TMI.2016.2528162.

[24] D. S. Kermany, M. Goldbaum, W. Cai, and M. A. Lewis.:Identifying Medical Diagnoses and Treatable Diseases by Image-Based Deep Learning Resource Identifying Medical Diagnoses and Treatable Diseases by Image-Based Deep Learning. pp. 1122–1131, 2018.

[25] K. Yasaka, H. Akai, A. Kunimatsu, S. Kiryu, and O. Abe.:Deep learning with convolutional neural network in radiology. Jpn. J. Radiol., vol. 36, no. 4, pp. 257–272, 2018, doi: 10.1007/s11604-018-0726-3.

[26] Y. Yu et al.:Deep learning enables automated scoring of liver fibrosis stages. no. October, pp. 1–10, 2018, doi: 10.1038/s41598-018-34300-2.

[27] M. Byra et al.:Transfer learning with deep convolutional neural network for liver steatosis assessment in ultrasound images. Int. J. Comput. Assist. Radiol. Surg., vol. 13, no. 12, pp. 1895–1903, 2018, doi: 10.1007/s11548-018-1843-2.

[28] A. Yamada et al.:Dynamic contrast-enhanced computed tomography diagnosis of primary liver cancers using transfer learning of pretrained convolutional neural networks: Is registration of multiphasic images necessary. Int. J. Comput. Assist. Radiol. Surg., vol. 14, no. 8, pp. 1295–1301, 2019, doi: 10.1007/s11548-019-01987-1

[29] K. He, X. Zhang, S. Ren, and J. Sun.:Deep residual learning for image recognition. Proceedings of the IEEE Computer Society Conference on Computer Vision and Pattern Recognition, 2016, vol. 2016-Decem, pp. 770–778, doi: 10.1109/CVPR.2016.90.

[30] T. A. Addissouky *et al.*, "Latest advances in hepatocellular carcinoma management and prevention through advanced technologies," *Egyptian Liver Journal*, vol. 14, no. 1. Springer Science and Business Media Deutschland GmbH, Dec. 01, 2024. doi: 10.1186/s43066-023-00306-3.

[31] N. Mizouri, "Deep learning neural network with transferlearning for liver cancer classiication Deep learning neural network with transfer learning for liver cancer classification," 2022, doi: 10.21203/rs.3.rs-2355564/v1.

[32] Mohamed Masoud1, Hoda Anwar Ibrahim1 and Kamel Hussein Rahouma2,"A comparative study of machine learning algorithms for diagnosis of hepatocellular carcinoma", Egyptian Computer Science Journal Vol. 46 No.2 September 2022 ISSN-1110-2586

[33] Liver segmentation – 3D-ircadb-01 - IRCAD.https://www.ircad.fr/research/data-sets/liver-segmentation-3d-ircadb-01/ (accessed Jun. 25, 2022).

[34] K. Kim.:A New Hyper Parameter of Hounsfield Unit Range in Liver Segmentation. vol. 0170, no. 3, pp. 103–111, 2020.

[35] Y. A. Labeeb.:Preprocessing Technique for Enhancing the DICOM Kidney Images. vol. 4, no. 08, pp. 836–841, 2015.

[36] S. H. Malik.:Contrast Enhancement and Smoothing of CT. March, 2015.

[37] Q. Jin, Z. Meng, C. Sun, H. Cui, and R. Su, "RA-UNet.: A Hybrid Deep Attention-Aware Network to Extract Liver and Tumor in CT Scans. vol. 8, no. December, pp. 1–15, 2020, doi: 10.3389/fbioe.2020.605132.

[38] J. Peng et al.:Residual convolutional neural network for predicting response of transarterial chemoembolization in hepatocellular carcinoma from CT imaging. Eur. Radiol., vol. 30, no. 1, pp. 413–424, 2020, doi: 10.1007/s00330-019-06318-1.

[39] E. Mocsari and S. S. Stone.:Colostral IgA, IgG, and IgM-IgA fractions as fluorescent antibody for the detection of the coronavirus of transmissible gastroenteritis. Am. J. Vet. Res., vol. 39, no. 9, pp. 1442–1446, 1978.

[40] M. Ahmad et al.:Deep Belief Network Modeling for Automatic Liver Segmentation. IEEE Access, vol. 7, pp. 20585–20595, 2019, doi: 10.1109/ACCESS.2019.2896961.

[41] Y. Yuan.:Hierarchical Convolutional-Deconvolutional Neural Networks for Automatic Liver and Tumor Segmentation. vol. i, pp. 3–6, 2017, [Online]. Available: http://arxiv.org/abs/1710.04540.

[42] G. Chlebus, H. Meine, J. H. Moltz, and A. Schenk.:Neural Network-Based Automatic Liver Tumor Segmentation With Random Forest-Based Candidate Filtering.pp. 5–8, 2017, [Online]. Available: http://arxiv.org/abs/1706.00842.

[43] D. Yang et al.:Automatic liver segmentation using an adversarial image-to-image network. in Lecture Notes in Computer Science (including subseries Lecture Notes in Artificial Intelligence and Lecture Notes in Bioinformatics), 2017, vol. 10435 LNCS, pp. 507–515, doi: 10.1007/978-3-319-66179-7_58.

[44] X. Li, H. Chen, X. Qi, Q. Dou, C. W. Fu, and P. A. Heng.:H-DenseUNet: Hybrid Densely Connected UNet for Liver and Tumor Segmentation from CT Volumes. IEEE Trans. Med. Imaging, vol. 37, no. 12, pp. 2663–2674, 2018, doi: 10.1109/TMI.2018.2845918.